

MOL #70938

**THE ROLE OF TRANSMEMBRANE DOMAIN 3 (TMIII) IN THE ACTIONS OF
ORTHOSTERIC, ALLOSTERIC AND ATYPICAL AGONISTS OF THE M₄
MUSCARINIC ACETYLCHOLINE RECEPTOR**

**Katie Leach, Anna E. Davey, Christian C. Felder, Patrick M. Sexton and Arthur
Christopoulos**

Drug Discovery Biology, Monash Institute of Pharmaceutical Sciences & Dept. of
Pharmacology, Monash University, Parkville, 3052, Victoria, Australia (KL, AED, PMS,
AC) and Eli Lilly and Co., Indianapolis, IN, 46285, USA (CCF)

MOL #70938

Running title: Structure-function studies of M₄ muscarinic receptors

Address correspondence to:

Prof. Arthur Christopoulos, Drug Discovery Biology, Monash Institute of Pharmaceutical Sciences, Parkville, 3052, Victoria, Australia. Tel: +613 9903 9067. Fax: +613 9903 9581.

Email: arthur.christopoulos@monash.edu

Number of text pages: 45

Number of tables: 4

Number of figures: 8

Number of references: 53

Number of words in the *Abstract*: 247

Number of words in the *Introduction*: 643

Number of words in the *Discussion*: 1343

Abbreviations: ACh, acetylcholine; C₇/3-phth, heptane-1,7-bis-(dimethyl-3'-phthalimidopropyl) ammonium bromide ; CHO, Chinese hamster ovary; DMEM, Dulbecco's modified Eagle medium; ELISA , Enzyme-linked Immunosorbent Assay; FBS, fetal bovine serum; GPCR, G protein-coupled receptor; LY2033298, 3-amino-5-chloro-6-methoxy-4-methyl-thieno[2,3-b]pyridine-2-carboxylic acid cyclopropylamide; mAChR, muscarinic acetylcholine receptor ; McN-A-343, 4-*I*-[3-chlorophenyl]carbamoyloxy)-2-butynyltrimethylammonium chloride NDMC, *N*-desmethylclozapine; [³H]NMS, [³H]-*N*-methylscopolamine; [³H]QNB, [³H]-quinuclidinyl benzilate; ; TM, transmembrane domain

MOL #70938

ABSTRACT

Despite the discovery of a diverse range of novel agonists and allosteric modulators of the M₄ muscarinic acetylcholine (ACh) receptor (mAChR), little is known about how such ligands activate the receptor. We used site-directed mutagenesis of conserved residues in TMIII, a key region involved in G protein-coupled receptor (GPCR) activation, to probe the binding and function of prototypical orthosteric mAChR agonists, allosteric modulators and “atypical” agonists. We found that most mutations did not affect the binding of the allosteric modulators, with the exception of W108^{3.28}A¹ and L109^{3.29}A (which may contribute directly to the interface between allosteric and orthosteric sites) and mutation D112^{3.32}N (which may cause a global disruption of a hydrogen bond network). Although numerous mutations affected signaling, we did not identify amino acids that were important for the functional activity of any one class of agonist (orthosteric, allosteric or atypical) to the exclusion of any others, suggesting that TMIII is key for transmission of stimulus irrespective of the agonist. We also identified two key residues, Trp-108^{3.28} and Asp-112^{3.32}, that are essential for the transmission of binding cooperativity between 3-amino-5-chloro-6-methoxy-4-methyl-thieno[2,3-b]pyridine-2-carboxylic acid cyclopropylamide (LY2033298) and ACh. Finally, we found that LY2033298 was able to rescue functionally impaired signaling of ACh at the majority of mutants tested in a manner that was inversely correlated with the ACh signaling efficacy, indicating that a key part of the mechanism of the positive cooperativity mediated by LY2033298 on the endogenous agonist involves a global drive of the receptor towards an active conformation.

MOL #70938

INTRODUCTION

A vast array of ligands, ranging from photons and ions to large glycoproteins, interact with cell-surface GPCRs; these mediate a plethora of physiological functions and comprise one of the largest families of drug targets in the genome (Hopkins and Groom, 2002). Given such importance, an understanding of the structural basis underlying ligand binding and activation of GPCRs is vital. Although a handful of high-resolution GPCR crystal structures have been solved in recent years, the process remains challenging and the current structures are mostly of inactive state receptors (Lodowski et al., 2009). Consequently, substantial insights into molecular events governing ligand action at GPCRs continue to be gained through structure-function analyses based on alternative approaches, such as mutagenesis.

The mAChRs are prototypical members of the biogenic amine Family A GPCRs, and have long served as a model system for understanding the structural basis of small molecule action at these receptors (Hulme et al., 2003). In recent years, there has been a particular resurgence of interest in mechanisms of mAChR activation due to the discovery of novel selective agonists and allosteric modulators of these receptors, especially for the M₁ and M₄ mAChR subtypes (Conn et al., 2009), which represent very attractive targets for the treatment of cognitive deficits associated with diseases such as schizophrenia (Chan et al., 2008; Jones et al., 2008). In contrast to the M₁ mAChR, however, relatively few mutational analyses have been performed on the M₄ mAChR, and thus the structural basis of the subtype-selectivity of novel allosteric modulators and selective agonists is not well established.

The conserved orthosteric site that binds the endogenous agonist, ACh, is located in the top third of the transmembrane helical bundle of the mAChRs, and is believed to utilize contacts provided

MOL #70938

by inward-facing residues in TM domains III – VII (Hulme et al., 2003). In particular, TMIII contains a number of residues that have been implicated in both the binding and activating mechanisms of the mAChRs by participating in a “global” activation switch that involves a separation of the cytoplasmic region of TMVI away from TMIII and TMVII (Altenbach et al., 1996; Farrens et al., 1996; Gether et al., 1997; Hubbell et al., 2003; Jensen et al., 2001), and movement of the extracellular region of TMVI towards TMIII and TMVII (Elling et al., 1999; Schwartz et al., 2006). Although we recently identified residues in the extracellular portions of the M₄ mAChR that also contribute to ligand-specific activation of the receptor (Nawaratne et al., 2010), the contribution of key TMIII residues in this receptor to the activation mediated by orthosteric and allosteric mAChR ligands remains undetermined.

The current study therefore aimed to provide insight into the role of TMIII on the binding and activation mechanisms used by different classes of M₄ mAChR ligands (Supplementary Figure 1). These include the prototypical orthosteric agonists, ACh and pilocarpine, the negative allosteric modulator, heptane-1,7-bis-(dimethyl-3'-phthalimidopropyl) ammonium bromide (C₇/3-phth), the novel allosteric agonist and modulator, LY2033298, and the functionally selective agonists, 4-*I*-[3-chlorophenyl]carbamoyloxy)-2-butynyltrimethylammonium chloride (McN-A-343) and *N*-desmethylozapine (NDMC). Although the basis of the functional selectivity of the latter two compounds remains undetermined, it has been attributed in the past to them interacting with an allosteric site (May et al., 2007a; Sur et al., 2003); in the case of McN-A-343, we have shown that its interaction with the M₂ mAChR, at least, is via a “bitopic” mode that involves concomitant binding to both the orthosteric and an allosteric site (Valant et al., 2008). It is currently unknown whether such a bitopic mechanism is operative at the M₄ mAChR, and thus both McN-A-343 and NDMC are referred to herein as “atypical” agonists.

MOL #70938

The availability of this diverse repertoire of small molecule orthosteric, allosteric and atypical ligands affords, for the first time, an unprecedented opportunity to delineate the role of TMIII in the processes of M₄ mAChR binding, activation and transmission of cooperativity between two topographically distinct binding domains.

MOL #70938

MATERIALS AND METHODS

Materials

Chinese hamster ovary (CHO) FlpIn cells were from Invitrogen (WI), Hygromycin B was purchased from Roche (Indianapolis, IN). Dulbecco's modified Eagle medium (DMEM) and fetal bovine serum (FBS) were from Gibco (Gaithersburg, MD) and JRH Biosciences (Lenexa, KS), respectively. Primers used for the generation of mutant receptors were purchased from Geneworks (Adelaide, South Australia). The AlphaScreen SureFire phospho-ERK1/2 reagents were kindly donated by Drs. Michael Crouch and Ron Osmond (TGR Biosciences, South Australia). AlphaScreen streptavidin donor beads and anti-IgG (protein A) acceptor beads, [³H]-quinuclidinyl benzilate ([³H]-QNB; specific activity, 52 Ci/mmol) and [³H]-N-methylscopolamine ([³H]-NMS; specific activity, 72 Ci/mmol) were purchased from PerkinElmer Life and Analytical Sciences (Waltham, MA). LY2033298 was synthesized in-house at Eli Lilly (Indianapolis, IN), whilst C₇/3-phth was synthesized in-house by Dr. Celine Valant at the Monash Institute of Pharmaceutical Sciences. All other chemicals were from Sigma Chemical Co. (St. Louis, MO).

Receptor mutagenesis and generation of cell lines

DNA encoding the human M₄ mAChR with a triple HA tag at its amino terminus was purchased from Missouri University of Science and Technology (<http://www.cdna.org>) and cloned into the Gateway destination vector, pEF5/frt/v5/dest, as described previously (Nawaratne et al., 2008). This construct was used to generate M₄ mAChR sequences with the desired amino acid substitutions using Quikchange™ site-directed mutagenesis (Stratagene) with primers shown in Supplementary Table 1. DNA constructs were transfected into FlpIn CHO cells (Invitrogen) for

MOL #70938

stable expression according to manufacturer's instructions. Cells were maintained in high glucose DMEM containing 10% FBS, 16 mM HEPES, and 400 µg/ml hygromycin B.

Radioligand binding assays

Cell membranes were prepared as described previously (Leach et al., 2010; Nawaratne et al., 2008). For equilibrium binding, cell membranes (50µg) were incubated in a final volume of 1ml binding buffer (20mM HEPES, 100mM NaCl, 10mM MgCl₂, 100µM GppNHp, pH 7.4) for 2 h at 37°C with [³H]QNB as described previously (Leach et al., 2010; Nawaratne et al., 2008); [³H]QNB was chosen for the equilibrium binding experiments because it retained appreciable affinity for most of the mutations studied, in contrast to an alternative (and commonly used) prototypical orthosteric antagonist, [³H]NMS. Radioligand dissociation was determined by equilibrating cell membranes (50µg/1ml; 1 h; 37°C) with 0.2nM (wild type M₄ mAChR) or 1nM (W108^{3.28}A and L109^{3.29}A) [³H]NMS in binding buffer prior to the addition of 10µl atropine (10µM) in the absence or presence of modulator using a reverse-time protocol. Receptor-bound radioligand was separated from free radioligand using rapid filtration with a Brandel harvester and radioactivity determined by liquid scintillation counting.

ERK1/2 phosphorylation assays

Cells were seeded at 40,000 cells per well into a transparent 96-well plate and grown overnight. Initial time course experiments were used to determine the time required to stimulate maximum ERK1/2 phosphorylation by each agonist and subsequent concentration response experiments were conducted by stimulating cells with agonist for 4 min. For interaction studies, where ACh-stimulated ERK1/2 phosphorylation was measured in the presence of LY2033298, the orthosteric

MOL #70938

agonist was added to cells immediately after the addition of LY2033298. Phosphorylated ERK1/2 was detected using an AlphaScreen assay as described previously (Nawaratne et al., 2008).

Enzyme-linked Immunosorbent Assay (ELISA)

Cells were seeded at 75,000 cells per well into a transparent 48-well plate and grown overnight. Cells were washed 3X with phosphate buffered saline (PBS; 137 mM NaCl, 2.7 mM KCl, 4.3 mM Na₂HPO₄ and 1.5 mM KH₂PO₄) and fixed with 4% paraformaldehyde for 15 min at 4°C prior to 2 more washes with PBS. Cells were blocked with 5% BSA for 45 min and incubated with rabbit anti-HA antibody (Abcam) for 1 h at 37°C. Cells were washed 3X with PBS and blocked for a further 15 min with 5% BSA. Cells were subsequently incubated with HRP-conjugated anti-rabbit IgG (Cell Signaling Technology) in PBS for 1 h at 37°C prior to 3X washes with PBS. The signal was developed using Sigma OPD tablets and the reaction was stopped by the addition of 3M HCl. Absorbance was read at 492nm using an Envision plate reader (PerkinElmer).

Data analysis

Radioligand dissociation kinetic experiments were fitted to a monoexponential decay equation (Motulsky and Christopoulos, 2004) and rate constants determined in the presence of LY2033298 were normalized to those determined in its absence. Competition binding curves between [³H]QNB and unlabelled orthosteric ligands were fitted to a one site binding model (Motulsky and Christopoulos, 2004). Inhibition experiments that utilized the allosteric

MOL #70938

modulators, LY2033298 or C₇/3-phth, were fitted to the following allosteric ternary complex model (Ehlert, 1988):

$$Y = \frac{B_{\max} [A]}{[A] + \left(\frac{K_A K_B}{\alpha' [B] + K_B} \right) \left(1 + \frac{[I]}{K_I} + \frac{[B]}{K_B} + \frac{\alpha [I][B]}{K_I K_B} \right)} \quad (1)$$

where Y is the specific radioligand binding, B_{max} is the total number of receptors, [A], [B] and [I] are the concentrations of radioligand, allosteric modulator, and unlabelled orthosteric ligand, respectively, K_A, K_B and K_I are the equilibrium dissociation constants of the radioligand, allosteric modulator and unlabelled orthosteric ligand, respectively and α' and α are the cooperativity factors between allosteric modulator and the radioligand or unlabelled orthosteric ligand, respectively. For binding experiments performed with C₇/3-phth vs [³H]QNB, [I] was set to 0 (i.e., no ACh was present in the experiment and the interaction was between C₇/3-phth and [³H]QNB only).

All ERK1/2 phosphorylation assays were analyzed using an operational model of allosterism and agonism according to Equation 2 (Leach et al., 2010; Leach et al., 2007):

$$E = \frac{E_m (\tau_A [A] (K_B + \alpha \beta [B]) + \tau_B [B] K_A)^n}{([A] K_B + K_A K_B + [B] K_A + \alpha [A][B])^n + (\tau_A [A] (K_B + \alpha \beta [B]) + \tau_B [B] K_A)^n} \quad (2)$$

where E_m is the maximum possible tissue response, [A] and [B] are the concentrations of orthosteric and allosteric ligands, respectively, K_A and K_B are the equilibrium dissociation constant of the orthosteric and allosteric ligands, respectively, τ_A and τ_B are operational measures of orthosteric and allosteric ligand efficacy, respectively, α is the binding cooperativity parameter between the orthosteric and allosteric ligand, and β denotes the allosteric effect of the modulator on the efficacy of the orthosteric agonist. When no allosteric modulator was present,

MOL #70938

the concentration of [B] was set to 0 and the model becomes identical to the original operational model of agonism described by Black and Leff (Black and Leff, 1983). Thus, in all instances, agonism is expressed in operational model terms. For the analysis to converge when an allosteric modulator was present, the binding cooperativity with ACh, α , was fixed to that determined separately in radioligand binding assays. In all instances, the equilibrium dissociation constant of each agonist was also fixed to that determined from the binding assays. Finally, to account for effects of the expression level of each of the different mutant receptors on the observed efficacy of each agonist, the B_{\max} values determined from saturation binding were used to normalize the $\text{Log}\tau$ values derived from the operational model analysis to what they would be if the mutant were expressed at the same level as the wild type receptor (Gregory et al., 2010); this corrected efficacy value is denoted as $\text{Log}\tau_C$.

All affinity, potency and cooperativity values were estimated as logarithms (Christopoulos, 1998) and statistical comparisons between values for agonists at each different mutant receptor was by one-way ANOVA using a Dunnett's multiple comparison post test to determine significant differences between mutant receptors and the wild type M_4 mAChR. A value of $P < 0.05$ was considered statistically significant.

MOL #70938

RESULTS

Rationale behind the choice of amino acid substitutions

A snake diagram of the M₄ mAChR is shown in Figure 1, highlighting the amino acid residues that were mutated in the current study. We have focused on residues conserved across all five mAChR subtypes located within TMIII because this region is vitally important for both the binding of orthosteric ligands, as well as activation of the receptor (Hulme et al., 2001; 2003). Very little is known, however, about the role of these residues in the actions of allosteric ligands.

Effects of TMIII substitutions on the affinity of orthosteric and atypical ligands

In all assays, the triple HA-tagged wild type human M₄ mAChR (referred to herein as WT) was compared to the untagged receptor to ensure that the pharmacology of the receptor was not altered by the tag. Although the presence of the HA tag caused a significant reduction in the number of [³H]QNB binding sites detected using saturation binding assays (untagged: 1.35 ± 0.18 pmol/mg protein, HA-tagged: 0.16 ± 0.03pmol/mg protein; n = 3-6), no significant differences were observed between the binding affinity of any of the ligands tested at the tagged and untagged receptor (data not shown). Thus, all subsequent receptor constructs were prepared with the triple HA tag.

As determined by [³H]QNB saturation binding analysis, the exchange of Asp-106^{3,26} for Ala, or Asp-129^{3,49} for Asn, led to a significant reduction in receptor expression compared to the WT, whereas substitution of Val-120^{3,40} for Ala resulted in a significant increase in receptor expression levels (Table 1). No [³H]QNB binding was detected following exchange of Asp-112^{3,32} or Tyr-113^{3,33} for Ala, although this likely reflects a dramatic inhibitory effect on orthosteric ligand affinity rather than receptor expression because a separate ELISA assay

MOL #70938

indicated that these latter two constructs were indeed expressed in our FlpIn CHO cells (Supplementary Fig. 2). No other amino acid substitutions had any significant effects on the expression level of the M₄ mAChR (Table 1).

In addition to substitution of Asp-112^{3.32} or Tyr-113^{3.33} with Ala, substantial effects were noted on ligand affinity for other receptor mutants. In particular, substituting Asp-112^{3.32} with Asn to eliminate the potential ionic interaction with the common ammonium cation of prototypical orthosteric mAChR ligands resulted in a large reduction in the binding affinity of both orthosteric and atypical ligands (Table 1; Figure 3). Elongation of the amino acid side chain while retaining the charge of Asp-112^{3.32}, by substitution with Glu, had a more selective effect, causing a large reduction in ACh affinity, a modest reduction in pilocarpine affinity, but no effect on the binding of [³H]QNB, McN-A-343 or NDMC (Table 1; Figure 2 and Figure 3). A considerable effect on ACh affinity was also observed following substitution of Leu-109^{3.29} for Ala, and smaller effects were observed for other ligands as well (Table 1; Figure 2 and Figure 3). Substitution of Ser-116^{3.36} or Asn-117^{3.37} for Ala had significant inhibitory effects on the binding affinity of ACh, but minimal to no effect on the affinity of any of the other ligands. In general, these findings are consistent with the important role these residues play in defining part of the orthosteric pocket for the endogenous agonist.

In agreement with recent findings at the M₂ mAChR (Gregory et al., 2010), the W108^{3.28}A mutant M₄ mAChR had opposing effects on ACh affinity (reduction) relative to that of the atypical ligand, NDMC (increase), suggesting that this residue is a key discriminator between the binding poses adopted by these ligands. A different profile was noted upon substitution of Val-120^{3.40} for Ala, which caused a modest decrease in the affinity of [³H]QNB and NDMC, but a

MOL #70938

modest increase in the affinity of ACh and pilocarpine. No significant differences were noted in ligand affinities at the D129^{3.49}E mutant, but removal of the charge (D129^{3.49}N) caused a modest increase in ACh affinity.

Effects of TMIII substitutions on the affinity of allosteric ligands

The interaction between the allosteric modulator, C₇/3-phth, and the orthosteric antagonist, [³H]QNB, is characterized by substantial negative cooperativity, and thus effects of amino acid substitutions on the binding of the modulator could be determined by application of a simple allosteric ternary complex model to the data. In contrast, the interaction between the allosteric ligand, LY2033298 and [³H]QNB, is neutrally cooperative (i.e., $\alpha' = 1$; Equation 1) (Leach et al., 2010; Nawaratne et al., 2008), and thus the effects of receptor mutations on the binding of the latter modulator were determined via analysis of the interaction between ACh and [³H]QNB in the presence of LY2033298 (Nawaratne et al., 2010).

Perhaps not unexpectedly, the majority of the mutations in TMIII did not have any significant effects on the affinity of the two allosteric modulators (Table 2; Figure 3), with a few notable exceptions. Specifically, allosteric ligand affinity was reduced at both the W108^{3.28}A and L109^{3.29}A mutant M₄ mAChRs (Table 2, Figures 3 and 4), suggesting that these two residues represent an interface between the prototypical orthosteric binding site and a more extracellular allosteric site; a previous study of the M₁ mAChR had identified a similar inhibitory effect of the W^{3.28}A on the binding of the allosteric modulator, gallamine (Matsui et al., 1995). Due to the indirect nature of the experiments used to determine mutational effects on LY2033298, we also utilized a second experimental paradigm for determining the potency of this modulator at the two

MOL #70938

mutants. Specifically, we took advantage of the ability of LY2033298 to allosterically retard the dissociation rate of the orthosteric antagonist, [³H]NMS (Leach et al., 2010), which enabled us to measure the LY2033298 concentration range over which this occurred at different receptor constructs (Figure 5A). Because the cooperativity between LY2033298 and [³H]NMS is also close to neutral at the M₄ mAChR (Leach et al., 2010) (Figure 5B), the potency (IC₅₀) determined in dissociation kinetic assays will be approximately equal to the K_B value of LY2033298 at the allosteric site (Lazareno and Birdsall, 1995); [³H]NMS was used instead of [³H]QNB for these experiments because the former antagonist has a much faster rate of dissociation than the latter, thus allowing determination of dissociation kinetics over a reasonable experimental time frame. Accordingly, there was a clear reduction in the potency of LY2033298 to slow [³H]NMS dissociation at both the W108^{3.28}A (pIC₅₀ 4.24 ± 0.07, n=3) and L109^{3.29}A (pIC₅₀ 4.28 ± 0.14, n=3) mutant M₄ mAChRs compared to the WT (pIC₅₀ 4.70 ± 0.07, n=3) (Figure 5), confirming the results of the equilibrium binding data and indicating that the affinity of LY2033298 for the allosteric site was indeed reduced.

A second surprising finding was that removal of the charge on Asp-112^{3.32} through substitution with Asn had a profound inhibitory effect on the affinity of C₇/3p_{th} while slightly enhancing the affinity of LY2033298 (Table 2; Figure 3, Supplementary Figure 3). Given the important role of this residue as a contact point for ACh and other orthosteric ligands, it is likely that the differential effect of mutation of Asp-112^{3.32} on allosteric ligand affinity represents an indirect conformational effect.

Residues in TMIII of the M₄ mAChR are involved in receptor activation by all classes of ligand

MOL #70938

We used ERK1/2 phosphorylation as a measure of agonist-stimulated receptor activity because this is a convergent pathway downstream of both G protein-dependent and -independent mechanisms. With the exception of C₇/3-phth, all ligands displayed some agonistic activity at this pathway. We identified a number of residues that contributed to the signaling of orthosteric, allosteric and atypical agonists, as quantified by the operational model Log τ _C values (Figure 6; Table 3). Mutations D106^{3.26}A, L109^{3.29}A, D112^{3.32}E and D112^{3.32}N, S116^{3.36}A and N117^{3.37}A were detrimental to the efficacy of all agonists tested. We did not identify any residues that contributed solely to the efficacy of one particular class of agonist (e.g. orthosteric, allosteric or atypical), but substitution of Val-120^{3.40} with Ala caused a significant decrease in the efficacy of ACh, LY2033298 and McN-A-343, whilst the efficacy of pilocarpine and NDMC was enhanced by this mutation. Similarly, exchange of Asp-129^{3.49} for Asn had no significant effect on the efficacy of ACh or LY2033298, yet the efficacy of McN-A-343, pilocarpine and NDMC was increased.

Residues in TMIII contribute to the transmission of cooperativity between the orthosteric and allosteric sites

The ability of an allosteric modulator to alter the function of an orthosteric ligand can be manifested as either changes in the binding affinity and/or changes in the signaling efficacy of the orthosteric ligand (May et al., 2007b). Thus, we determined the extent to which different amino acid residues in TMIII were involved in the transmission of binding cooperativity (α') between C₇/3-phth and [³H]QNB, and both binding cooperativity (α) and efficacy modulation (β) between LY2033298 and ACh; allosteric effects of C₇/3-phth on ACh could not be

MOL #70938

investigated due to the very high negative cooperativity between this modulator and the agonist (not shown).

Two mutations, namely W108^{3.28}A and L109^{3.29}A, had substantial effects on the binding cooperativity between each of the modulators and their respective orthosteric interactants (Table 2; Figure 4). With regards to W108^{3.28}A, it was of note that both the negative cooperativity between C₇/3-phth and [³H]QNB, and the positive cooperativity between LY2033298 and ACh, were blunted in each instance (Table 2), suggesting that this residue is not only important for modulator binding affinity, but also for the optimal transmission of cooperative effects. In contrast, L109^{3.29}A had opposing effects on cooperativity, i.e., increasing the positive cooperativity between LY2033298 and ACh while reducing the negative cooperativity between C₇/3-phth and [³H]QNB. D106^{3.26}A also had a selective (blunting) effect on the negative cooperativity between C₇/3-phth and [³H]QNB. The greatest measurable effect on the binding cooperativity between LY2033298 and ACh was observed at the D112^{3.32}E and D112^{3.32}N mutants, where a large reduction in the ability of LY2033298 to potentiate ACh binding affinity was observed (Figure 4, Table 2). Although the cooperativity between C₇/3-phth and [³H]QNB at the D112^{3.32}N mutant could not be determined accurately due to the pronounced reduction of modulator affinity at this construct (Supplementary Figure 3), the data were consistent with retention of substantial negative cooperativity at the mutant because a significant reduction in the binding of [³H]QNB was noted in the presence of high C₇/3-phth concentrations (Supplementary Figure 3), suggesting that the principal effect of the mutation is on modulator affinity rather than cooperativity.

MOL #70938

To determine the effects of amino acid substitutions on the ability of LY2033298 to modulate the signaling efficacy of ACh, we performed functional interaction studies using ERK1/2 phosphorylation as a measure of agonist-mediated receptor activation and fitted the data to an operational model of allosterism and agonism (Equation 2) (Leach et al., 2010; Leach et al., 2007). An internal check of the robustness of the analysis was the excellent correlation between $\text{Log}\tau_c$ estimates obtained for ACh or LY2033298 in experiments when the ligands were tested on their own as agonists (Table 3) compared to when they were co-administered together in the interaction studies (Table 4; Figure 7); for the ACh comparison, $r^2 = 0.89$ and for the LY2033298 comparison, $r^2 = 0.95$.

With the exception of the D112^{3.32}A, D112^{3.32}N and Y113^{3.33}A mutations, where little or no response was observed to ACh in both the absence or presence of LY2033298, the key finding from the functional interaction experiments was that the allosteric modulator was able to rescue ACh function to varying extents at all other mutant receptors, with significant increases in the strength of the allosteric modulation of ACh efficacy (β) noted at the L109^{3.29}A, D112^{3.32}E and S116^{3.36}A mutant receptors (Table 4, Figure 7). Indeed, there was a significant inverse correlation ($r^2 = 0.71$) between the observed signaling efficacy of ACh and the ability of LY2033298 to potentiate ACh-mediated signaling, where lower ACh $\text{Log}\tau_c$ values (more impaired orthosteric agonist signaling) were associated with higher $\text{Log}\beta$ values for the interaction (Figure 8). This finding indicates that a key part of the mechanism of the positive cooperativity mediated by LY2033298 on the endogenous agonist involves a global drive of the receptor towards an active conformation, irrespective of the nature of mutational impairment in TMIII residues.

MOL #70938

DISCUSSION

The mAChRs are an important model system for understanding structure-function relationships at Family A GPCRs due to the growing number of ligands with novel modes of action being identified for these receptors. In addition to Asp-129^{3,49}, located near the cytosolic end of TMIII as part of the highly conserved (E)/DRY activation motif, the current study focused predominantly on amino acid residues that contribute to the top (extracellular-facing) half of TMIII of the M₄ mAChR, which remains less characterized than other mAChR subtypes despite emerging as an exciting drug target for cognitive disorders such as schizophrenia (Chan et al., 2008). The fact that mutations in this region of the receptor had substantial effects on orthosteric, allosteric and atypical mAChR ligands highlights the pivotal role that TMIII plays in mechanisms of activation and transmission of allosteric effects at the M₄ mAChR. Given the high degree of conservation of these residues across the mAChR and biogenic GPCR families, it is likely that some of the mechanisms inferred from our study will be operative at other GPCRs.

As expected, the majority of TMIII mutations did not substantially affect the binding affinity of the allosteric modulators, C₇/3-phth and LY2033298, with the exception of W108^{3,28}A, L109^{3,29}A and D112^{3,32}N. Trp-108^{3,28} and Leu-109^{3,29} are predicted to lie near the junction of TMIII and the extracellular entrance to the orthosteric binding pocket, and it is thus reasonable to hypothesize that these residues may contribute to lining the “bottom” of a more extracellularly-located allosteric binding domain. This hypothesis is also supported by our recent finding that C₇/3-phth and LY2033298 interact in an apparently competitive manner at the M₄ mAChR (Leach et al., 2010), suggesting that they share overlapping binding regions on the receptor. The effect of removing the charge on Asp-112^{3,32} was unexpected due to the fact that this residue is the key counter-ion that interacts with the ammonium headgroup of ACh (Curtis et al., 1989;

MOL #70938

Kurtenbach et al., 1990; Spalding et al., 1994). However, Asp-112^{3.32} is believed to participate in a hydrogen bond network with key residues near the top TMVII, a region that has previously been implicated in contributing to the binding pocket of prototypical modulators such as C_{7/3}-phth (Huang et al., 2005; Matsui et al., 1995; May et al., 2007a; Prilla et al., 2006; Voigtlander et al., 2003), and disruption of this network may account for the deleterious effects on C_{7/3}-phth binding.

In contrast, the prototypical orthosteric ligands and atypical agonists utilized in this study were generally characterized by reduced binding affinity at a variety of the TMIII mutants with a few notable exceptions. The first was McN-A-343, which exhibited no significant difference in binding affinity at any mutant except the key D112^{3.32}N M₄ mAChR construct. This finding is consistent with prior studies of the M₂ mAChR, where McN-A-343 was unaffected by key orthosteric site mutations, in agreement with our hypothesis that this compound adopts a bitopic binding mode that extends up from Asp^{3.32} towards the extracellular loop regions (Gregory et al., 2010; Valant et al., 2008). The second exception was the modest increases in affinity noted for NDMC at the W108^{3.28}A mutant, for ACh and pilocarpine at the V120^{3.40}A mutant, and for ACh at the D129^{3.49}N mutant, respectively. The first of these observations is consistent with what has been noted for NDMC at the equivalent mutation introduced into the M₂ mAChR (Gregory et al., 2010), but is the opposite to the small decrease in its binding affinity at the equivalent mutation of the M₁ mAChR (Lebon et al., 2009), suggesting that NDMC adopts a slightly different binding pose at the even-numbered mAChRs compared to the M₁ mAChR.

It was also interesting to note that substitution of Ser-116^{3.36} and Asn-117^{3.37} to Ala caused a large reduction in the binding affinity of ACh, but not in the affinity of any of the other ligands

MOL #70938

tested, indicating that ACh adopts a unique binding pose in comparison to the other agonists. It is unclear whether these residues are direct contact points for ACh, because although Ser-116^{3.36} is predicted to face directly into the core of the orthosteric binding pocket (Han et al., 2005), Asn-117^{3.37} is located below the predicted orthosteric binding site. Therefore, Asn-117^{3.37} may serve to stabilize an important receptor conformation that is essential for ACh binding but not for any of the other ligands tested.

With regards to mutational effects on ligand signaling efficacy, it was of particular note that we did not identify any amino acids that were important for the functional activity of one particular class of agonist (orthosteric, allosteric or atypical) to the exclusion of any others, suggesting that the location of the agonist binding site does not necessarily govern a unique activation mechanism following agonist binding, and that there are some global receptor conformations that are favored by all agonists. Furthermore, with the exception of ligand-specific effects of the V120^{3.40}A and D129^{3.49}N mutations, the rest of the mutations introduced into TMIII were generally deleterious to receptor activation. The substitution of Val-120^{3.40} with Ala caused a significant increase in the signaling efficacy of pilocarpine, suggesting that even prototypical orthosteric ligands can sense different conformations compared to the endogenous ligand for the receptor. In contrast, the removal of the charge on Asp-129^{3.49} caused an increase in the efficacy of all agonists tested, with the interesting exceptions of the endogenous orthosteric ligand, ACh, and the allosteric agonist, LY2033298. The general view of mechanisms involving Asp^{3.49} in Family A GPCR activation is that it forms an important hydrogen bond interaction with Arg^{3.50}, which itself interacts with Glu^{6.30} in the formation of a key “ionic lock”; disruption of this lock is proposed to be part of the activation mechanism for many GPCRs (Schwartz et al., 2006). This could explain why compounds such as pilocarpine, McN-A-343 and NDMC displayed enhanced

MOL #70938

signaling at this mutant receptor, assuming that the mutation placed the receptor in a partially active state with respect to ERK1/2 phosphorylation. However, prior studies at the M₁ and M₅ mAChRs have found minimal effects of the D^{3.49}N mutation on the efficacy of ACh itself (Burstein et al., 1998; Lu et al., 1997), which is also in agreement with our current study at the M₄ mAChR, suggesting that this mechanism need not be universal. It is noteworthy that the signaling efficacy of the allosteric agonist, LY2033298, was also completely insensitive to the D^{3.49}N mutation. Overall, these findings are concordant with recent experiments on the β_2 adrenergic receptor, which showed that diverse agonists disrupt a different combination of molecular interactions responsible for stabilizing that receptor's inactive state (Yao et al., 2006).

Given that a key aim of our study was to also quantify the effects of TMIII mutations on the cooperativity between co-bound orthosteric and allosteric ligands on the M₄ mAChR, we can reveal for the first time two key residues required for the transmission of binding cooperativity between LY2033298 and ACh. Trp-108^{3.28} and Asp-112^{3.32} were essential for the ability of LY2033298 to potentiate the binding affinity of ACh. Intriguingly, however, even though the binding cooperativity was almost abolished at the D112^{3.32}E mutant, the allosteric effect on signaling between ACh and LY203329 was retained. In fact, at the L109^{3.29}A, D112^{3.32}E and S116^{3.36}A mutants, an *increase* in efficacy modulation between LY2033298 and ACh was observed. This may be expected where ACh-mediated receptor signaling events are significantly impaired by an amino acid substitution if LY2033298 can restore them to functional receptors. It also highlights that an important, yet often underappreciated, mechanism of allosteric modulation is a “re-setting” of energy barriers governing global transitions between receptor states by an

MOL #70938

allosteric modulator that subsequently facilitates (or hinders) the interaction with an orthosteric ligand.

In conclusion, the present study has identified conserved amino acid residues in the key TMIII domain that play a role in the binding, signaling and transmission of cooperativity in a diverse range of orthosteric, allosteric and atypical mAChR ligands. We have shown that although common activation switches are used by all classes of M₄ mAChR agonist, some subtle differences exist between the intramolecular interactions that are altered following the binding of different agonists.

ACKNOWLEDGEMENTS

We would like to thank Dr. Celine Valant for the synthesis of C₇/3-phth and Drs. Michael Crouch and Ron Osmond (TGR Biosciences) for the generous donation of AlphaScreen SureFire phospho-ERK1/2 reagents.

MOL #70938

AUTHORSHIP CONTRIBUTIONS

Participated in research design: Leach, Davey, Sexton and Christopoulos

Conducted experiments: Leach and Davey

Contributed new reagents or analytic tools: Felder

Performed data analysis: Leach, Davey and Christopoulos

Wrote or contributed to the writing of the manuscript: Leach, Davey, Felder, Sexton
and Christopoulos

Other: Christopoulos and Sexton acquired funding for the research.

MOL #70938

REFERENCES

- Altenbach C, Yang K, Farrens DL, Farahbakhsh ZT, Khorana HG and Hubbell WL (1996) Structural features and light-dependent changes in the cytoplasmic interhelical E-F loop region of rhodopsin: a site-directed spin-labeling study. *Biochemistry (Mosc)* **35**(38):12470-12478.
- Black JW and Leff P (1983) Operational models of pharmacological agonism. *Proceedings of the Royal Society of London Series B, Containing papers of a Biological character* **220**(1219):141-162.
- Burstein ES, Spalding TA and Brann MR (1998) The second intracellular loop of the m5 muscarinic receptor is the switch which enables G-protein coupling. *J Biol Chem* **273**(38):24322-24327.
- Chan WY, D LM, Bose S, S NM, J MW, Thompson RC, Christopoulos A, Lazareno S, Birdsall NJ, Bymaster FP and Felder CC (2008) Allosteric modulation of the muscarinic M4 receptor as an approach to treating schizophrenia. *Proc Natl Acad Sci U S A* **105**:10978–10983.
- Christopoulos A (1998) Assessing the distribution of parameters in models of ligand-receptor interaction: to log or not to log. *Trends Pharmacol Sci* **19**(9):351-357.
- Conn PJ, Jones CK and Lindsley CW (2009) Subtype-selective allosteric modulators of muscarinic receptors for the treatment of CNS disorders. *Trends Pharmacol Sci* **30**(3):148-155.

MOL #70938

- Curtis CA, Wheatley M, Bansal S, Birdsall NJ, Eveleigh P, Pedder EK, Poyner D and Hulme EC (1989) Propylbenzylcholine mustard labels an acidic residue in transmembrane helix 3 of the muscarinic receptor. *J Biol Chem* **264**(1):489-495.
- Ehlert FJ (1988) Estimation of the affinities of allosteric ligands using radioligand binding and pharmacological null methods. *Mol Pharmacol* **33**(2):187-194.
- Elling CE, Thirstrup K, Holst B and Schwartz TW (1999) Conversion of agonist site to metal-ion chelator site in the beta(2)-adrenergic receptor. *Proc Natl Acad Sci U S A* **96**(22):12322-12327.
- Farrens DL, Altenbach C, Yang K, Hubbell WL and Khorana HG (1996) Requirement of rigid-body motion of transmembrane helices for light activation of rhodopsin. *Science* **274**(5288):768-770.
- Gether U, Lin S, Ghanouni P, Ballesteros JA, Weinstein H and Kobilka BK (1997) Agonists induce conformational changes in transmembrane domains III and VI of the beta2 adrenoceptor. *EMBO J* **16**(22):6737-6747.
- Gregory KJ, Hall NE, Tobin AB, Sexton PM and Christopoulos A (2010) Identification of orthosteric and allosteric site mutations in M2 muscarinic acetylcholine receptors that contribute to ligand-selective signaling bias. *J Biol Chem*.
- Han SJ, Hamdan FF, Kim SK, Jacobson KA, Bloodworth LM, Li B and Wess J (2005) Identification of an agonist-induced conformational change occurring adjacent to the ligand-binding pocket of the M(3) muscarinic acetylcholine receptor. *J Biol Chem* **280**(41):34849-34858.
- Hopkins AL and Groom CR (2002) The druggable genome. *Nat Rev Drug Discov* **1**(9):727-730.

MOL #70938

- Huang XP, Prilla S, Mohr K and Ellis J (2005) Critical amino acid residues of the common allosteric site on the M2 muscarinic acetylcholine receptor: more similarities than differences between the structurally divergent agents gallamine and bis(ammonio)alkane-type hexamethylene-bis-[dimethyl-(3-phthalimidopropyl)ammonium]dibromide. *Mol Pharmacol* **68**(3):769-778.
- Hubbell WL, Altenbach C, Hubbell CM and Khorana HG (2003) Rhodopsin structure, dynamics, and activation: a perspective from crystallography, site-directed spin labeling, sulfhydryl reactivity, and disulfide cross-linking. *Adv Protein Chem* **63**:243-290.
- Hulme EC, Lu ZL, Bee M, Curtis CA and Saldanha J (2001) The conformational switch in muscarinic acetylcholine receptors. *Life Sci* **68**(22-23):2495-2500.
- Hulme EC, Lu ZL, Saldanha JW and Bee MS (2003) Structure and activation of muscarinic acetylcholine receptors. *Biochem Soc Trans* **31**(Pt 1):29-34.
- Jensen AD, Guarnieri F, Rasmussen SG, Asmar F, Ballesteros JA and Gether U (2001) Agonist-induced conformational changes at the cytoplasmic side of transmembrane segment 6 in the beta 2 adrenergic receptor mapped by site-selective fluorescent labeling. *J Biol Chem* **276**(12):9279-9290.
- Jones CK, Brady AE, Davis AA, Xiang Z, Bubser M, Tantawy MN, Kane AS, Bridges TM, Kennedy JP, Bradley SR, Peterson TE, Ansari MS, Baldwin RM, Kessler RM, Deutch AY, Lah JJ, Levey AI, Lindsley CW and Conn PJ (2008) Novel selective allosteric activator of the M1 muscarinic acetylcholine receptor regulates amyloid processing and produces antipsychotic-like activity in rats. *J Neurosci* **28**(41):10422-10433.

MOL #70938

Kurtenbach E, Curtis CA, Pedder EK, Aitken A, Harris AC and Hulme EC (1990)

Muscarinic acetylcholine receptors. Peptide sequencing identifies residues involved in antagonist binding and disulfide bond formation. *J Biol Chem* **265**(23):13702-13708.

Lazareno S and Birdsall NJ (1995) Detection, quantitation, and verification of allosteric interactions of agents with labeled and unlabeled ligands at G protein-coupled receptors: interactions of strychnine and acetylcholine at muscarinic receptors. *Mol Pharmacol* **48**(2):362-378.

Leach K, Loiacono RE, Felder CC, McKinzie DL, Mogg A, Shaw DB, Sexton PM and Christopoulos A (2010) Molecular Mechanisms of Action and In Vivo Validation of an M(4) Muscarinic Acetylcholine Receptor Allosteric Modulator with Potential Antipsychotic Properties. *Neuropsychopharmacology* **35**(4):855-869.

Leach K, Sexton PM and Christopoulos A (2007) Allosteric GPCR modulators: taking advantage of permissive receptor pharmacology. *Trends Pharmacol Sci* **28**(8):382-389.

Lebon G, Langmead CJ, Tehan BG and Hulme EC (2009) Mutagenic mapping suggests a novel binding mode for selective agonists of M1 muscarinic acetylcholine receptors. *Mol Pharmacol* **75**(2):331-341.

Lodowski DT, Angel TE and Palczeski K (2009) Comparative analysis of GPCR crystal structures. *Photochem Photobiol* **85**: 425-430.

Lu ZL, Curtis CA, Jones PG, Pavia J and Hulme EC (1997) The role of the aspartate-arginine-tyrosine triad in the m1 muscarinic receptor: mutations of aspartate 122

MOL #70938

- and tyrosine 124 decrease receptor expression but do not abolish signaling. *Mol Pharmacol* **51**(2):234-241.
- Matsui H, Lazareno S and Birdsall NJ (1995) Probing of the location of the allosteric site on m1 muscarinic receptors by site-directed mutagenesis. *Mol Pharmacol* **47**(1):88-98.
- May LT, Avlani VA, Langmead CJ, Herdon HJ, Wood MD, Sexton PM and Christopoulos A (2007a) Structure-function studies of allosteric agonism at M2 muscarinic acetylcholine receptors. *Mol Pharmacol* **72**(2):463-476.
- May LT, Leach K, Sexton PM and Christopoulos A (2007b) Allosteric modulation of G protein-coupled receptors. *Annu Rev Pharmacol Toxicol* **47**:1-51.
- Motulsky H and Christopoulos A (2004) *Fitting models to biological data using linear and nonlinear regression. A practical guide to curve fitting*. Oxford University Press, New York.
- Nawaratne V, Leach K, Felder CC, Sexton PM and Christopoulos A (2010) Structural determinants of allosteric agonism and modulation at the M4 muscarinic acetylcholine receptor: identification of ligand-specific and global activation mechanisms. *J Biol Chem* **285**(25):19012-19021.
- Nawaratne V, Leach K, Suratman N, Loiacono RE, Felder CC, Armbruster BN, Roth BL, Sexton PM and Christopoulos A (2008) New insights into the function of M4 muscarinic acetylcholine receptors gained using a novel allosteric modulator and a "designer receptor exclusively activated by a designer drug" (DREADD). *Mol Pharmacol* **74**(4):1119-1131.

MOL #70938

- Prilla S, Schrobang J, Ellis J, Holtje HD and Mohr K (2006) Allosteric interactions with muscarinic acetylcholine receptors: complex role of the conserved tryptophan M2422Trp in a critical cluster of amino acids for baseline affinity, subtype selectivity, and cooperativity. *Mol Pharmacol* **70**(1):181-193.
- Schwartz TW, Frimurer TM, Holst B, Rosenkilde MM and Elling CE (2006) Molecular mechanism of 7TM receptor activation--a global toggle switch model. *Annu Rev Pharmacol Toxicol* **46**:481-519.
- Spalding TA, Birdsall NJ, Curtis CA and Hulme EC (1994) Acetylcholine mustard labels the binding site aspartate in muscarinic acetylcholine receptors. *J Biol Chem* **269**(6):4092-4097.
- Sur C, Mallorga PJ, Wittmann M, Jacobson MA, Pascarella D, Williams JB, Brandish PE, Pettibone DJ, Scolnick EM and Conn PJ (2003) N-desmethyloclozapine, an allosteric agonist at muscarinic 1 receptor, potentiates N-methyl-D-aspartate receptor activity. *Proc Natl Acad Sci U S A* **100**(23):13674-13679.
- Valant C, Gregory KJ, Hall NE, Scammells PJ, Lew MJ, Sexton PM and Christopoulos A (2008) A novel mechanism of G protein-coupled receptor functional selectivity. Muscarinic partial agonist McN-A-343 as a bitopic orthosteric/allosteric ligand. *J Biol Chem* **283**(43):29312-29321.
- Voigtlander U, Jöhren K, Mohr M, Raasch A, Trankle C, Buller S, Ellis J, Holtje HD and Mohr K (2003) Allosteric site on muscarinic acetylcholine receptors: identification of two amino acids in the muscarinic M2 receptor that account entirely for the M2/M5 subtype selectivities of some structurally diverse allosteric ligands in N-methylscopolamine-occupied receptors. *Mol Pharmacol* **64**(1):21-31.

MOL #70938

Yao X, Parnot C, Deupi X, Ratnala VR, Swaminath G, Farrens D and Kobilka B (2006)

Coupling ligand structure to specific conformational switches in the beta2-adrenoceptor. *Nat Chem Biol* **2**(8):417-422.

MOL #70938

FOOTNOTES

This work was supported by the National Health and Medical Research Council of Australia [519461]. Arthur Christopoulos is a Senior, and Patrick Sexton a Principal, Research Fellow of the NHMRC.

Numbered footnotes:

¹ Ballesteros and Weinstein numbers are provided (in superscript) to indicate relative position of residues within the transmembrane domain.

FINANCIAL DISCLOSURES

AC is a Consultant for Johnson & Johnson and Alchemia. CCF is an employee of Eli Lilly and Co.

REPRINT REQUESTS TO

Prof. Arthur Christopoulos

Drug Discovery Biology

Monash Institute of Pharmaceutical Sciences

Parkville, 3052, Victoria, Australia.

Tel: +613 9903 9067. Fax: +613 9903 9581.

Email: arthur.christopoulos@monash.edu

MOL #70938

FIGURE LEGENDS

Figure 1 Snake diagram of the M₄ mAChR. Highlighted in dark grey are the amino acid residues mutated in this study.

Figure 2 Mutations in TMIII differentially alter the equilibrium dissociation constant of orthosteric M₄ ligands. Bars represent the change in pK_B of each ligand at the mutant receptor relative to the wild-type receptor, determined from equilibrium radioligand binding assays. Data are mean ± s.e.m from at least three experiments performed in triplicate. *N/D* indicates that there was no detectable binding and * represents a significant difference to wild-type, $p < 0.05$, one-way analysis of variance, Dunnett's post-test.

Figure 3 Mutations in TMIII have differential effects on the equilibrium dissociation constant of allosteric and atypical M₄ ligands. Bars represent the change in pK_B of each ligand at the mutant receptor relative to the wild-type receptor, determined either from equilibrium radioligand binding assays or from non-equilibrium radioligand dissociation assays. Data are mean ± s.e.m. from at least three experiments performed in triplicate. *N/D* indicates that there was no detectable binding and * represents a significant difference to wild-type, $p < 0.05$, one-way analysis of variance, Dunnett's post-test.

MOL #70938

Figure 4 Radioligand binding interaction studies reveal mutations that alter the cooperativity and/or binding affinity of LY2033298. The competition between a K_A -equivalent concentration of [^3H]QNB and a fixed concentration of ACh, which inhibited approximately 20% [^3H]QNB binding (100 μM at W108^{3.28}, 300 μM at L109^{3.29}A, 10mM at D112^{3.32}N and 1mM at D112^{3.32}E) was determined in the presence of increasing concentrations of LY2033298 at the indicated mAChR constructs. The curves drawn through the points represent the best global fit of an allosteric ternary complex model (Equation 1) to each pair of datasets (ACh competition of [^3H]QNB binding and the IC_{20} concentration of ACh in the presence of LY2033298), with the cooperativity between LY2033298 and [^3H]QNB (α') fixed to a value of 1. Data points represent the s.e.m. of at least three experiments performed in triplicate.

Figure 5 [^3H]NMS dissociation kinetic studies confirm that the W108^{3.28}A and L109^{3.29}A mutations reduce the binding affinity of LY2033298. Concentration-effect relationships for LY2033298 on the dissociation rate of [^3H]NMS at the wild type, W108^{3.28}A or L109^{3.29}A mutants. Data represent mean \pm s.e.m. from three experiments performed in duplicate.

Figure 6 Agonist efficacy is differentially modified by TMIII mutations. Bars represent the difference in $\text{Log}\tau_C$ of each agonist, derived from an operational model of agonism (Equation 2), relative to the wild-type receptor value for that agonist. Data represent the mean \pm s.e.m of at least three experiments performed in triplicate. *No response* indicates that there was no detectable response and * represents a significant

MOL #70938

difference to the wild type receptor, $p < 0.05$, one-way analysis of variance, Dunnett's post-test.

Figure 7 **LY2033298 rescues ACh efficacy at inactivating mutations.** Peak levels of pERK1/2 were assessed as described under "Experimental Procedures" and normalised to the response elicited by 10% FBS. The curves drawn through the points for data at the WT, W108^{3.28}, L109^{3.29} and D112^{3.32}E constructs represent the best global fit of an operational model of allosterism (Equation 2) to each family of datasets, with the affinity of each agonist fixed to the pK_B value determined in separate binding assays (Table 1). Curves drawn through the points for data at the D112^{3.32}N construct represent the fit of each curve to a simple Hill equation. Data points represent the mean \pm s.e.m of at least three experiments performed in triplicate

Figure 8 **The ability of LY2033298 to potentiate ACh activity correlates well with the efficacy of ACh at each mutant.** ACh $\text{Log}\tau_C$ and $\text{Log}\beta$ values between ACh and LY2033298 were determined from fitting pERK1/2 interaction data at the WT and mutant receptors to an operational model of allosterism (Equation 2), as described under "Experimental Procedures". The line drawn through the points represents the best fit of a linear regression analysis to the data, where r^2 represents the correlation between $\text{Log}\tau_C$ and $\text{Log}\beta$.

Table 1 **Equilibrium binding parameter estimates for ligands at M₄ mAChR**

constructs. Values represent the mean ± s.e.m. from at least three separate experiments performed in triplicate

	B_{max} (fmol / mg protein)^a	pK_A^b	pK_B^c	
	[³H]QNB		ACh	Pilocarpine
M₄ WT	159 ± 28	10.45 ± 0.12	4.89 ± 0.02	5.01 ± 0.13
M₄ D106^{3.26}A	41 ± 20*	9.70 ± 0.06*	3.95 ± 0.09*	4.24 ± 0.16*
M₄ W108^{3.28}A	111 ± 21	9.77 ± 0.13*	4.01 ± 0.06*	4.59 ± 0.07
M₄ L109^{3.29}A	107 ± 31	9.12 ± 0.10*	3.11 ± 0.09*	4.22 ± 0.11*
M₄ D112^{3.32}N	183 ± 12	8.44 ± 0.09*	< 2	< 3
M₄ D112^{3.32}E	152 ± 39	10.34 ± 0.10	3.19 ± 0.02*	4.16 ± 0.09*
M₄ S116^{3.36}A	158 ± 18	10.51 ± 0.07	3.61 ± 0.10*	5.09 ± 0.23
M₄ N117^{3.37}A	260 ± 48	9.95 ± 0.10	3.64 ± 0.04*	4.46 ± 0.04
M₄ V120^{3.40}A	264 ± 34*	9.41 ± 0.16*	5.63 ± 0.05*	5.95 ± 0.03*
M₄ D129^{3.49}E	77 ± 40	10.14 ± 0.13	5.04 ± 0.07	4.53 ± 0.19
M₄ D129^{3.49}N	54 ± 9*	10.11 ± 0.17	5.54 ± 0.10*	5.08 ± 0.09

^a Maximum density of binding sites.

^b Negative logarithm of the radioligand equilibrium dissociation constant.

^c Negative logarithm of the unlabeled ligand equilibrium dissociation constant.

* Significantly different (*p* < 0.01) from WT value as determined by one way ANOVA

with Dunnett's post-hoc test.

Table 2 **Allosteric modulator equilibrium binding parameters.** Values represent the mean \pm s.e.m. from at least three separate experiments performed in triplicate.

	C₇/3-phth		LY2033298	
	pK_B^a	Logα' (α')^b	pK_B^a	Logα (α)^c
M₄ WT	5.58 \pm 0.03	-1.88 \pm 0.02 (0.01)	5.21 \pm 0.17	1.85 \pm 0.18 (71)
M₄ D106^{3.26}A	5.66 \pm 0.07	-1.19 \pm 0.12* (0.06)	5.29 \pm 0.11	1.51 \pm 0.15 (32)
M₄ W108^{3.28}A	4.83 \pm 0.14*	-1.14 \pm 0.13* (0.07)	4.24 \pm 0.07*	1.23 \pm 0.01* (17)
M₄ L109^{3.29}A	4.89 \pm 0.18*	-1.03 \pm 0.19* (0.09)	4.28 \pm 0.14*	2.54 \pm 0.10* (347)
M₄ D112^{3.32}N	3.64 \pm 0.17*	N/D	5.79 \pm 0.20*	0.74 \pm 0.08* (5)
M₄ D112^{3.32}E	5.30 \pm 0.01	-1.69 \pm 0.07 (0.02)	5.56 \pm 0.13	0.39 \pm 0.11* (2)
M₄ S116^{3.36}A	5.70 \pm 0.04	-2.09 \pm 0.11 (0.01)	5.12 \pm 0.08	1.54 \pm 0.05 (35)
M₄ N117^{3.37}A	5.29 \pm 0.05	-1.85 \pm 0.14 (0.01)	5.30 \pm 0.15	1.57 \pm 0.13 (37)
M₄ V120^{3.40}A	5.27 \pm 0.04	-1.38 \pm 0.04 (0.04)	5.41 \pm 0.10	1.83 \pm 0.11 (68)

M₄D129^{3,49}E	5.19 ± 0.14	-1.51 ± 0.17	5.59 ± 0.12	1.61 ± 0.16 (41)
		(0.03)		
M₄D129^{3,49}N	5.16 ± 0.09	-1.41 ± 0.08	5.37 ± 0.20	1.86 ± 0.22 (72)
		(0.04)		

^a Negative logarithm of the allosteric modulator equilibrium dissociation constant.

^b Logarithm of the cooperativity factor for the interaction between C_{7/3}-phth and [³H]QNB; antilogarithms are shown in parentheses.

^c Logarithm of the cooperativity factor for the interaction between LY2033298 and ACh; antilogarithms are shown in parentheses.

N/D Not determined

* Significantly different ($p < 0.05$) from WT value as determined by one way ANOVA with Dunnett's post-hoc test.

Table 3 Coupling efficiency ($\text{Log}\tau_c$) parameters of ligands at M_4 mAChR

constructs. Values represent the mean \pm s.e.m. from at least three separate experiments performed in triplicate.

	$\text{Log}\tau_c$ (τ_c)			
	ACh	Pilocarpine	LY2033298	McN-A-
M₄ WT	2.09 \pm 0.09 (123)	-0.93 \pm 0.08 (0.1)	1.37 \pm 0.08 (23)	0.84 \pm 0.1
M₄ D106^{3,26}A	0.60 \pm 0.22* (4)	NR	NR	NR
M₄ W108^{3,28}A	1.77 \pm 0.11 (59)	NR	NR	NR
M₄ L109^{3,29}A	1.23 \pm 0.11* (17)	NR	NR	NR
M₄ D112^{3,32}N	NR	NR	NR	NR
M₄ D112^{3,32}E	-1.20 \pm 0.74* (0.06)	NR	NR	NR
M₄ S116^{3,36}A	1.19 \pm 0.15* (15)	NR	0.02 \pm 0.11* (1)	NR
M₄ N117^{3,37}A	1.14 \pm 0.09* (14)	NR	-0.19 \pm 0.19* (0.7)	-0.93 \pm 0.19
M₄ V120^{3,40}A	1.50 \pm 0.13* (32)	0.33 \pm 0.10* (2)	0.88 \pm 0.12* (8)	0.01 \pm 0.19
M₄ D129^{3,49}E	1.29 \pm 0.20* (19)	NR	0.72 \pm 0.18* (5)	0.43 \pm 0.3
M₄ D129^{3,49}N	2.38 \pm 0.15 (240)	0.45 \pm 0.27* (3)	1.34 \pm 0.14 (22)	1.87 \pm 0.21

^a Logarithm of the corrected operational efficacy parameter, τ_c , determined via nonlinear regression of the concentration-response data to an operational model of agonism; antilogarithms are shown in parentheses.

NR No response.

* Significantly different ($p < 0.05$) from WT value as determined by one way ANOVA with Dunnett's post-hoc test.

Table 4 **Operational allosteric ternary complex model parameters for the functional interaction between ACh and LY2033298.** Parameter values are the mean \pm s.e.m. from at least three experiments performed in triplicate and analysed according to Equation 3.

	Logβ (β)^a	Logτ_C ACh (τ_C)
M₄ WT	0.90 \pm 0.03 (8)	1.84 \pm 0.12 (69)
M₄ D106^{3.26}A	0.80 \pm 0.17 (6)	1.24 \pm 0.11 (17)
M₄ W108^{3.28}A	1.16 \pm 0.20 (14)	1.49 \pm 0.17 (31)
M₄ L109^{3.29}A	1.43 \pm 0.14* (27)	1.17 \pm 0.14 (15)
M₄ D112^{3.32}N	N/D	N/D
M₄ D112^{3.32}E	2.26 \pm 0.16* (182)	-0.80 \pm 0.16* (0.2)
M₄ S116^{3.36}A	1.43 \pm 0.14* (27)	0.82 \pm 0.17* (7)
M₄ N117^{3.37}A	1.27 \pm 0.11 (19)	0.80 \pm 0.27* (6)
M₄ V120^{3.40}A	0.80 \pm 0.19 (6)	1.47 \pm 0.11 (30)
M₄ D129^{3.49}E	0.90 \pm 0.09 (8)	1.45 \pm 0.24 (28)
M₄ D129^{3.49}N	1.04 \pm 0.23(11)	2.56 \pm 0.39 (363)

^a Logarithm of the allosteric effect on orthosteric agonist efficacy (β).

^b Logarithm of the corrected operational efficacy parameter, τ_C .

^c Log τ_C for LY2033298 was fixed to -1000 (i.e., τ_C approaches 0) due to the lack of efficacy of LY2033298.

N/D Not determined

* Significantly different ($p < 0.05$) from WT value as determined by one way ANOVA with Dunnett's post-hoc test.

Figure 1

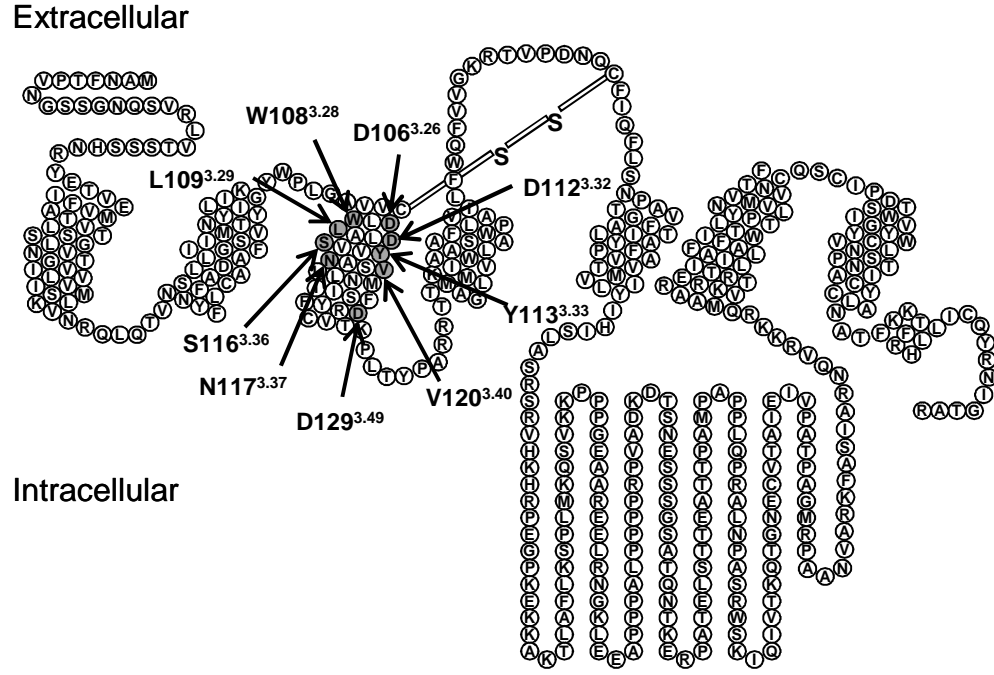


Figure 2

ΔpK_B

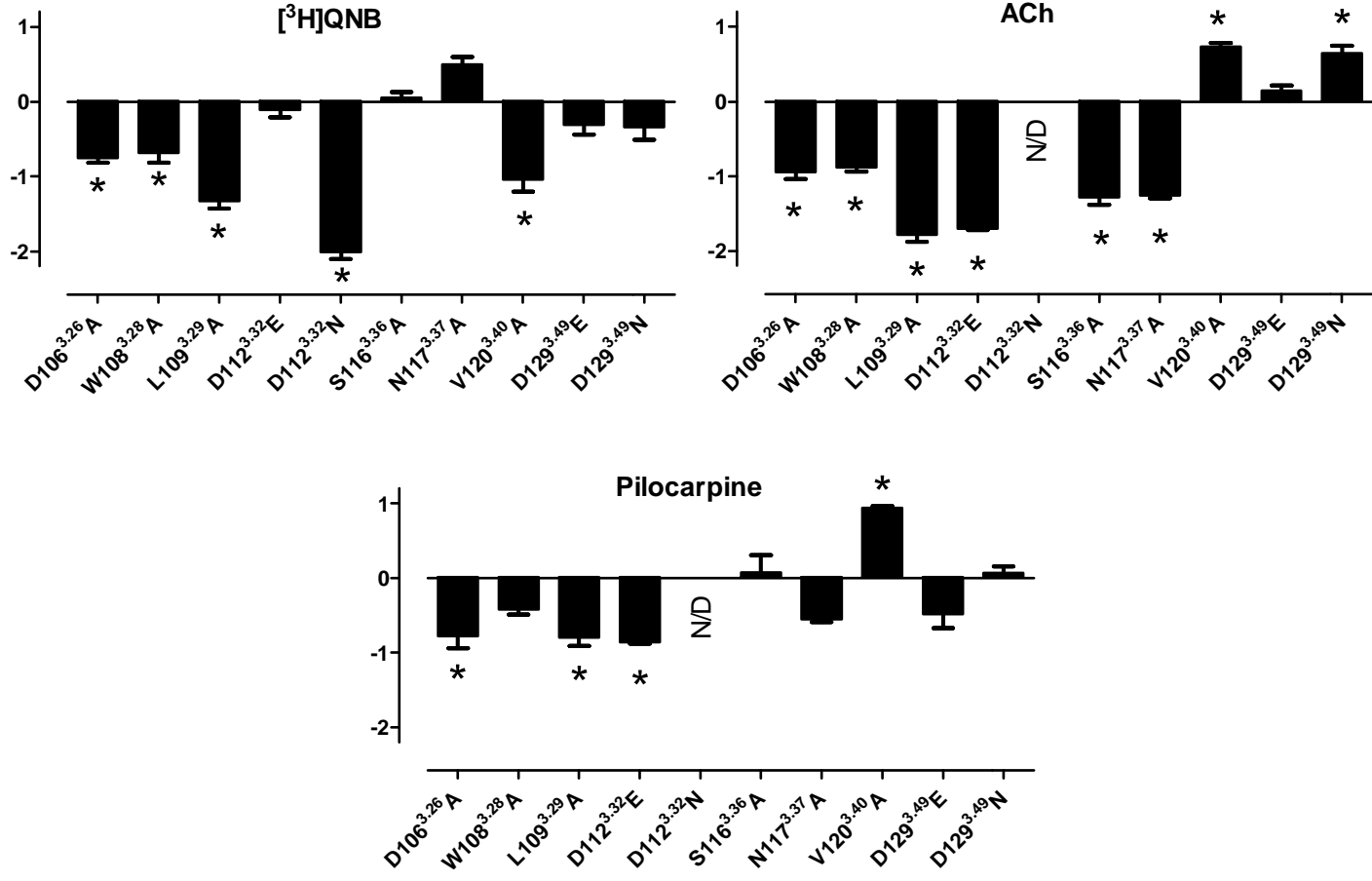


Figure 3

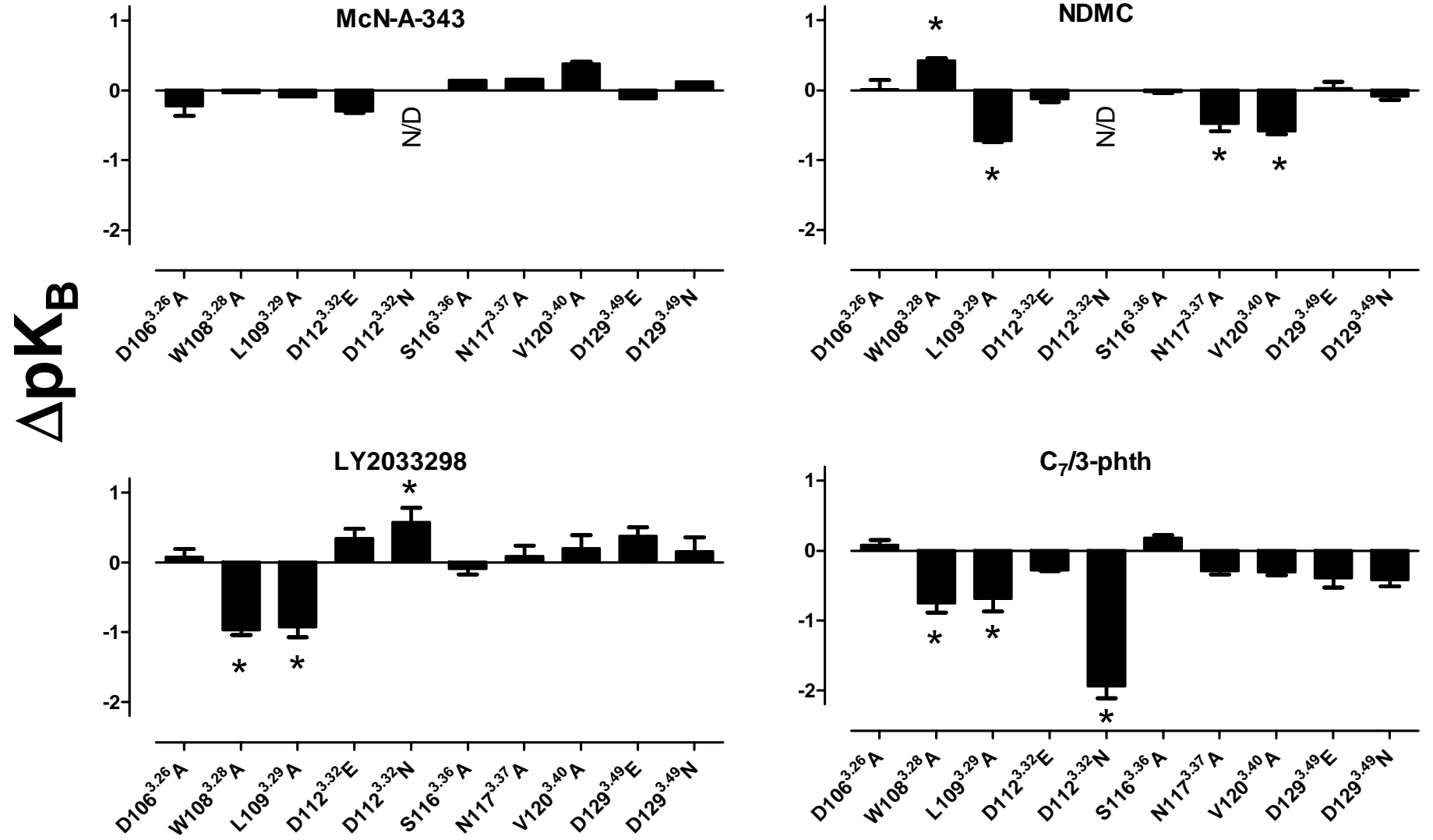


Figure 4

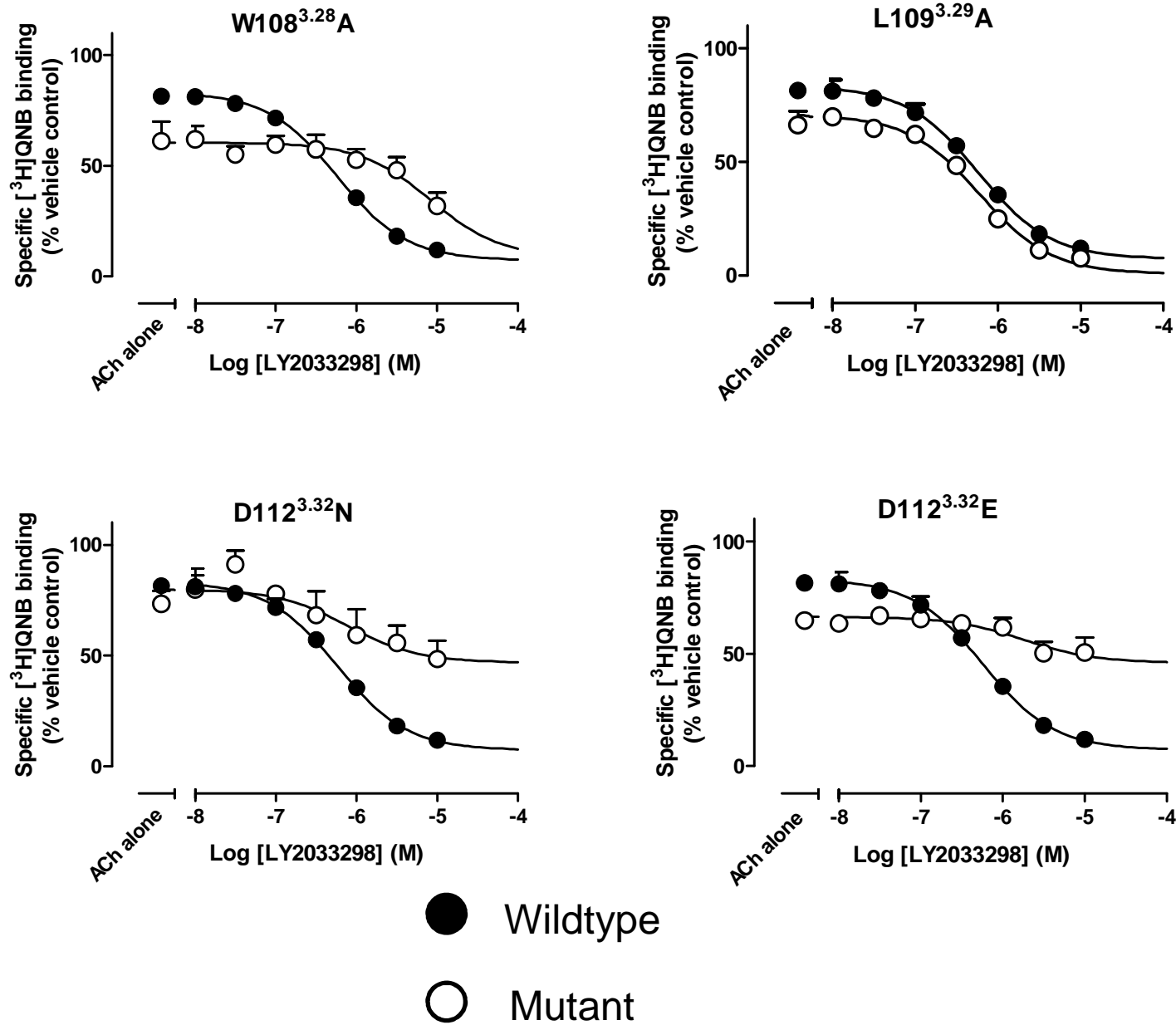


Figure 5 A

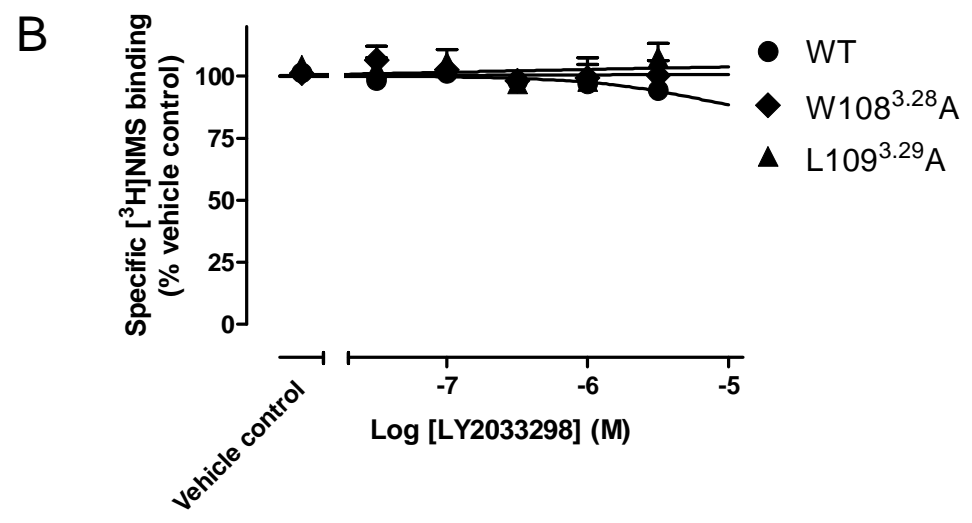
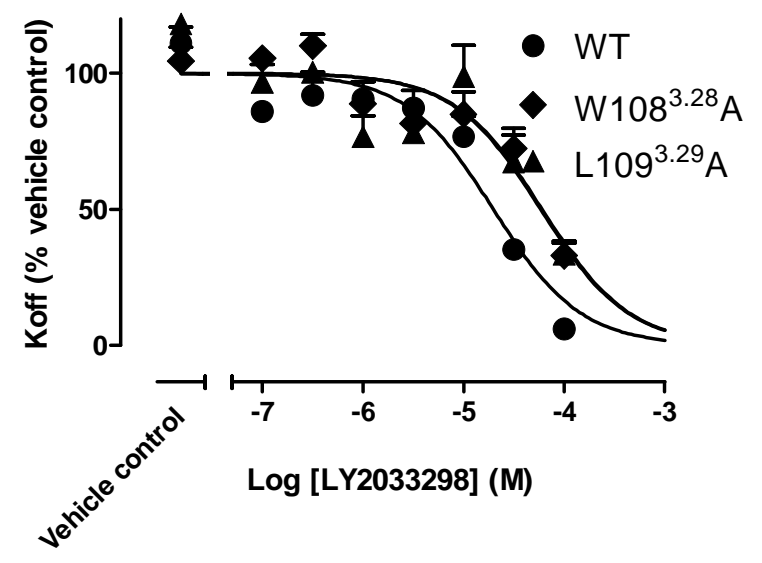


Figure 6

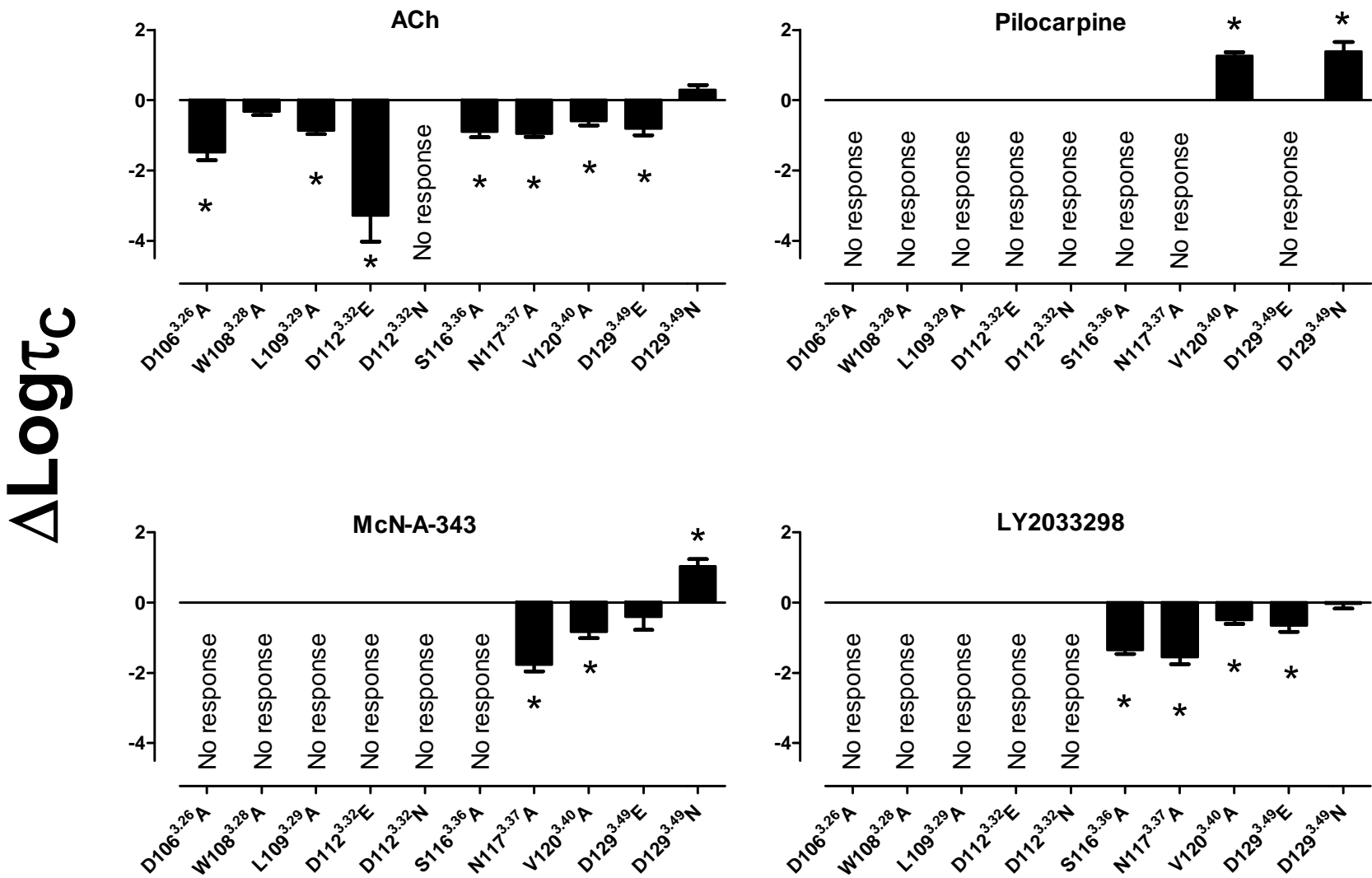


Figure 7

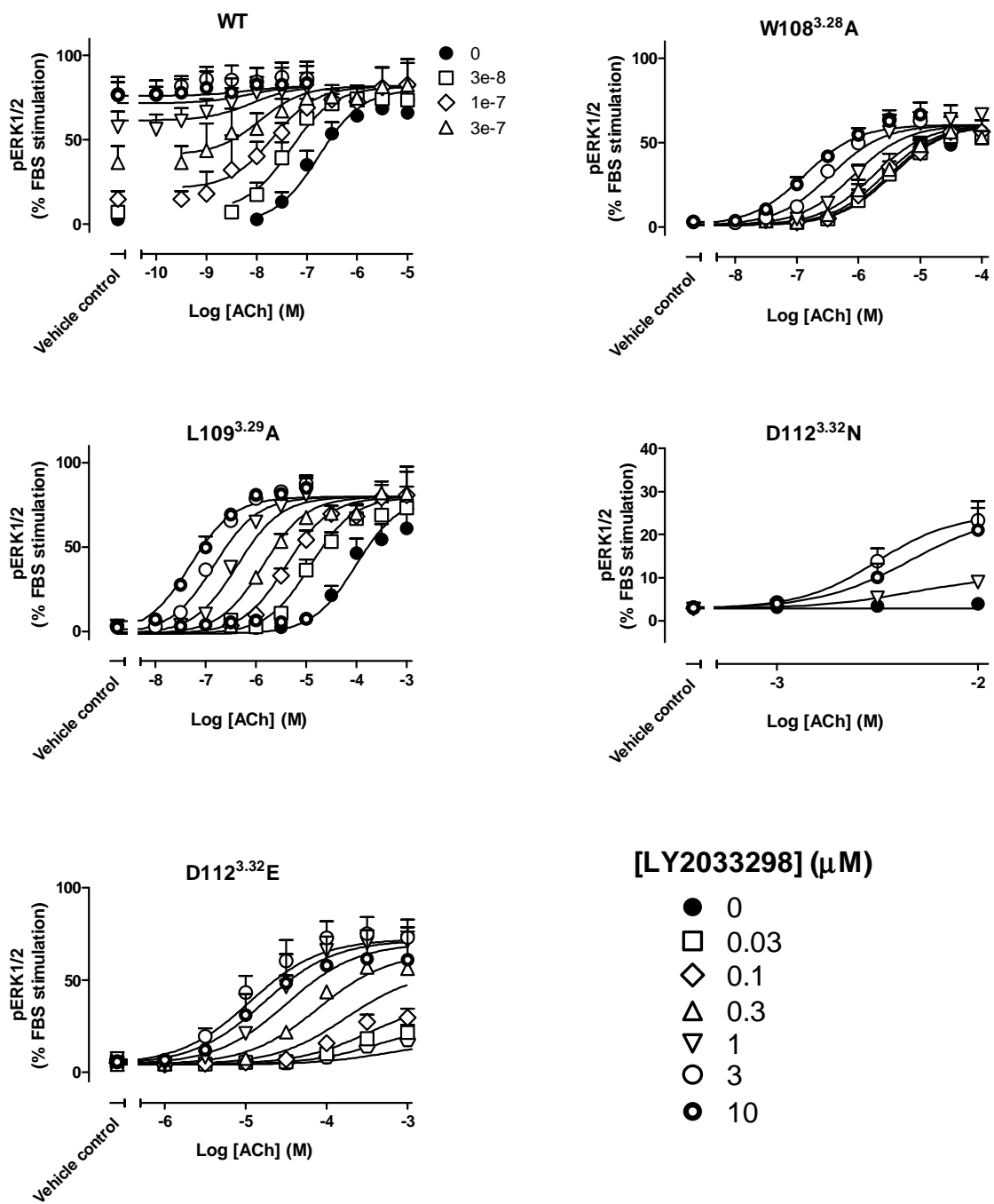


Figure 8

